CRYSTAL GROWTH & DESIGN

ACS AuthorChoice

Article

pubs.acs.org/crystal

Morphologies in Solvent-Annealed Clotrimazole Thin Films Explained by Hansen-Solubility Parameters

Heike M. A. Ehmann,[†] Andreas Zimmer,[†] Eva Roblegg,[†,‡] and Oliver Werzer*[,†]

[†]Institute of Pharmaceutical Sciences, Department of Pharmaceutical Technology, Karl-Franzens University Graz, 8010 Graz, Austria

[‡]Research Center Pharmaceutical Engineering GmbH, 8010 Graz, Austria

ABSTRACT: The induction of different crystal morphologies is of crucial importance for many applications. In this work, the preparation of various crystal morphologies within clotrimazole films on glass substrates is demonstrated. Amorphous clotrimazole thin films were transformed via vapor annealing into crystalline structures; highly monodisperse/multidisperse crystallites, spherulite, or dendritic structures were obtained as the solvent was exchanged. X-ray diffraction experiments reveal that the same polymorph is present for all samples but with varying texture. The achieved morphologies are explained in terms of Hansen-solubility parameters and vapor pressures; thus, the different morphologies and crystal orientations can be explained by solvent—solid interaction strengths within the thin film samples.

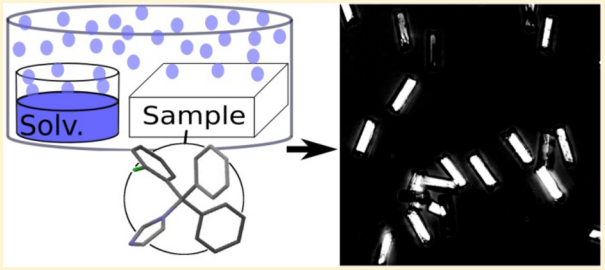

INTRODUCTION

Many newly developed active pharmaceutical ingredients (APIs) or drug molecules suffer from low aqueous solubility and belong therefore to the Biopharmaceutics Classification System (BCS) class II or IV.[1] Various approaches are demonstrated to achieve enhanced solubility; modification of particle size and co-crystallization among others are quite effective approaches for the promotion of in vitro dissolution and systemic adsorption.[2−4] In addition, the crystalline structure and the morphology are important parameters that influence the dissolution behavior.[2] While amorphous solid states are favorable in terms of solubility and dissolution rate, they often lack long term stability resulting in undesired crystallization on storage.[5,6] Thus, crystals are preferable in solid state pharmaceutical formulations. Further, APIs are often able to pack in various different crystalline arrangements[7,8] with each polymorph having different physiochemical and therapeutic properties.[9] Besides the solid state crystalline structure, the morphology has a great impact on the dissolution behavior.[3] For instance, the same amount of API in a dendritic structure dissolves faster compared to a single crystal due to the significantly larger surface area, which, according to Noyes−Whitney, increases the dissolution rate.[1,10] Within manufacturing processes, a demand for fast and reproducible crystallization is present. However, the time required to achieve crystalline structures strongly depends on the API in use.[1] Caffeine or phenytoin crystals spontaneously form on the removal of the solvent,[11] while the fast solvent removal in ibuprofen samples results in amorphous structures which transform into crystalline structures after several days.[12] In addition, the route of crystallizations is of importance, as for instance, fast crystallization in a single step provides reduced processing energies and production times rather than recrystallization from melts.[12]

Another approach is the usage of API loaded surfaces which allows systemic adsorption through topical or buccal routes from patches or nanoparticle surfaces.[13] Typically, the API is deposited onto a carrier material such as cellulose or a plaster which then aids in the therapeutic action.[14,15] The usage of supporting materials requires deeper knowledge of API—surface interaction for optimized formulations. At surfaces, crystallization is typically distinct resulting in altered polymorphs or morphologies compared to bulk crystallization from saturated solutions. There are examples[16−19] where certain polymorphs and morphologies are only present at the surface, which are classified as surface induced or mediated structures.[19]

Within this study, enhanced crystallization rate and the induction of various morphologies of an initial amorphous clotrimazole film at a solid substrate are demonstrated. Clotrimazole is used in many pharmaceutical formulations due to its antifungal activity, and a detailed description of its therapeutic efficacy can be found elsewhere.[20−25] The deposition of clotrimazole via fast solvent removal results in amorphous films.[26] Typically, the rearrangement of the molecules requires up to 10 days for the achievement of crystallization at ambient conditions, which in terms of manufacturing means enhanced costs.[27] In this work, the crystallization of clotrimazole during solvent annealing is investigated after a short period of time. Solvent annealing is known to effectively induce preferred polymorphic phases and morphologies within thin films.[28−30] In this "simple" technique,

Received: December 13, 2013
Revised: January 17, 2014
Published: February 10, 2014

   dx.doi.org/10.1021/cg401859p | *Cryst. Growth Des.* 2014, 14, 1386−1391

a sample is in contact with the vapor phase of a solvent, allowing interactions of the API and solvent molecules. Adsorbing solvent molecules promote molecule movement and/or rearrangement allowing crystallization to take place. It will be demonstrated that various morphologies can be induced by the exchange of solvents and are investigated by X-ray diffraction and optical microscopy. According to Hansen,[31] the interaction strength of each solvent is a result of dispersive, polar, and H-bonding interactions. Within this work, the Hansen-solubility parameters (HSPs) are used as an estimate for solvent interaction strength with clotrimazole thin films and the supporting silica substrate. It will be demonstrated that this set of parameters allows explaining the crystal formation in clotrimazole thin films.

MATERIALS & METHODS

Clotrimazole powder of pharmaceutical grade was purchased from Gatt-Koller GmbH (Austria) and used without further treatment. For the experiments, organic solvents including toluene (TOL), *p*-xylene (XYL), acetone (DMK), isopropanol (IPA), ethanol (EtOH), methanol (MeOH), tetrahydrofuran (THF), and acetonitrile (MeCN) were purchased from various sources in spectroscopic grade and used without further purification.

As substrates, glass slides (Carl Roth, Munich, Germany) were cut to 2.5 × 2.5 cm^2 pieces and cleaned in acetone, ethanol and a 0.1 M NaOH solution, respectively, in an ultrasonic bath. After treatment, the slides were rinsed with Milli-Q water and finally dried under a nitrogen stream.

Thin amorphous films of clotrimazole were obtained by spin coating[32] a 4.0 wt % clotrimazole−toluene solution onto the glass slides at a speed of 25 rps for 30 s, which resulted in homogeneous clotrimazole layers. Solvent annealing was performed by placing the clotrimazole films next to an open glass vessel containing the solvent and were enclosed together (see Figure 1). This results in a solvent vapor atmosphere in the vessel, and direct contacts of the liquid solvents with the samples are prevented. Solvent annealing times of 60 h at 25 °C were used for all investigations. This represents a quarter of the "normal" crystallization time which is typically needed at ambient conditions.[1] Selected samples were investigated at elevated temperatures of 70 °C under vacuum treatment (10^{-6} mbar) or solvent vapor.

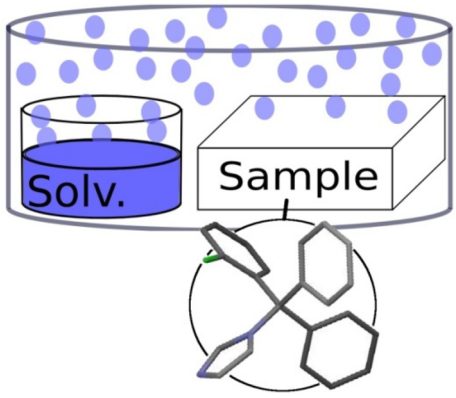

Figure 1. Scheme of the solvent annealing equipment and the structure of clotrimazole (bottom).

Drop casted films were prepared from toluene as well as *p*-xylene by dropping 100 μL of a 1.0 wt % solution onto 2.5 × 2.5 cm^2 glass substrates. The samples were covered with a Petri dish, which slowed the evaporation.

Optical microscopy was performed with an Axiovert 40 CFL polarization microscope in transmission mode and images were taken with a high resolution digital camera. The polarization setup utilizes an analyzer module Pol ACR P&C for transmitted light and a second polarizer, which is mounted before the light transmits through the sample. The last unit (polarizer) can be rotated to study bifringent (90°) as well as non-bifringent structures. In the course of this work, the polarizer was set to an angle of 85° to study both the amorphous domains as well as the crystalline regions simultaneously. The magnification of the used Zeiss LD Plan-NEOFLUAR 20x/0.4 Ph2 Korr objective was 20×.

X-ray diffraction measurements were performed with a Siemens D500 powder diffractometer in Bragg−Brentano configuration.[33] The radiation was provided by a copper sealed tube (wavelength 0.154 nm), and the beam was guided through a slit system. A secondary graphite monochromator was used prior the scintilization detector. Within such a setup, peak intensities correspond to netplanes aligned parallel to the surface.

Contact angle measurements were performed using the OCA15+ solution of dataphysics. Three different test liquids (namely, water, formamide, and diiodomethane) were dropped on the surface with a volume of 10 μL per drop. The sessile drop investigations with the semipolar formamide and the apolar diiodomethane partially dissolved the clotrimazole thin film. Hence, only the water contact angle is used to describe the hydrophobicity of the amorphous thin film.

RESULTS

All thin films of clotrimazole were prepared by spin coating from a single toluene solution onto the glass slides to minimize impacts of the preparation process on the crystal formation. The clotrimazole film had a thickness of about 140 nm and surface roughness of about 0.4 nm (determined by X-ray reflectivity; data not shown). Investigations with optical microscopy and X-ray diffraction reveal that the films prepared from toluene prior to solvent annealing are of a purely amorphous nature. Investigations on such a film, stored at ambient conditions, after a period of 60 h showed no differences compared to the as-prepared films; that is, crystallization did not take place in this time frame. Similarly, heat treating at 70 °C for 60 h under a vacuum (10^{-6} mbar) reveals a similar behavior; that is, heating to this temperature did not change the crystalline properties and the sample remained amorphous. The energy or mobility of the molecules was not sufficient to adapt a favorable crystalline conformation. Literature shows that a time frame of up to 10 days at ambient conditions is required to achieve crystallization of such a film.[1]

In Figure 2, the various clotrimazole morphologies obtained on vapor annealing in different solvents are shown. A film, water vapor annealed for 60 h, shows the formation of spherulite-like structures (see Figure 2a), while water vapor annealing at enhanced temperatures of 70 °C results in the formation of elongated crystallites with an extension up to 550 μm (Figure 2b). Using MeOH vapor at room temperature leads to an intermediate situation with elongated crystals (mean size 75 × 23 μm^2) flanked by spherulite-like structures (Figure 2c). In other alcohol vapors such as EtOH and IPA, large quadratic single crystals form as the films were exposed for 60 h (Figure 2d,e) but with the spherulites being absent. A mean square diameter of 70 and 100 μm is observed for EtOH and IPA, respectively. Similarly, a XYL vapor causes clotrimazole to assemble in single crystalline rods. However, other than with the alcohol samples, the crystals are uniform and are of significantly reduced size (28 × 8 μm^2). The change of the solvent to TOL results in a drastic change of the morphology; some rodlike structures are present, but the majority of the crystalline fractions show dendritic-like morphologies (see Figure 2g). These dendritic structures are even more pronounced within the samples which were vapor annealed in DMK and MeCN (Figure 2h,i).

dx.doi.org/10.1021/cg401859p | *Cryst. Growth Des.* 2014, 14, 1386−1391

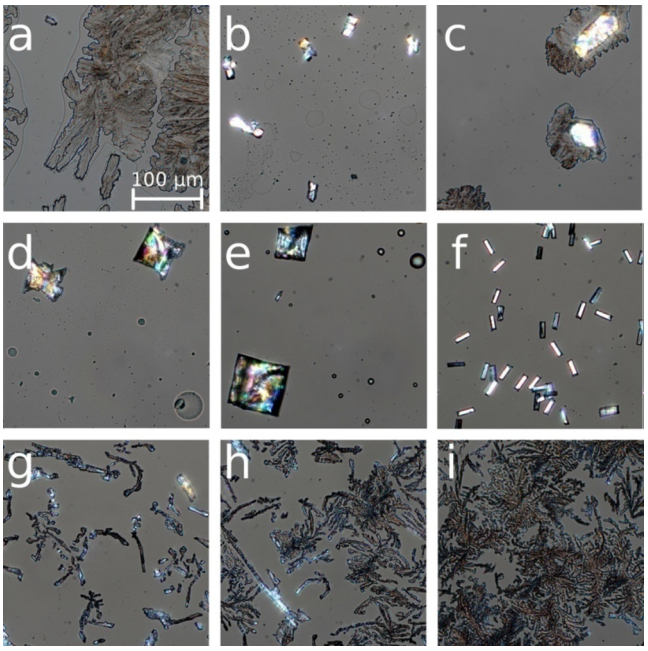

Figure 2. Optical microscope images (polarizer set to 85°) of clotrimazole thin films solvent annealed in water (a), water in an oven (70 °C) (b), methanol (c), ethanol (d), isoporpanol (e), *p*-xylene (f), toluene (g), acetone (h), and acetonitrile (i) atmospheres for 60 h.

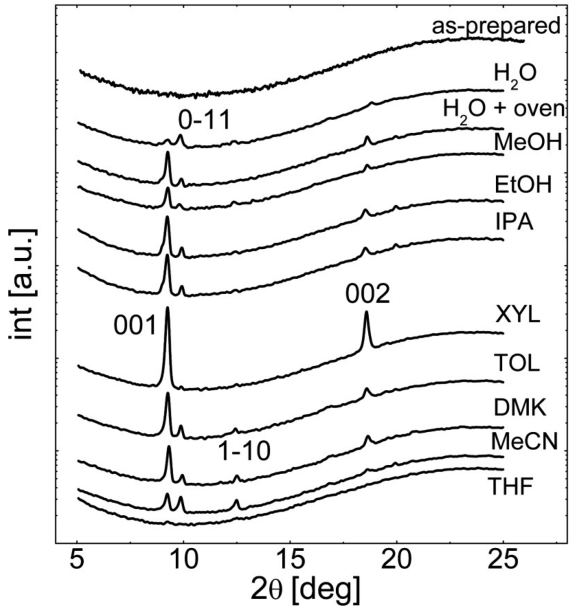

Figure 3. X-ray diffraction patterns of clotrimazole thin film (as prepared) as well as after vapor annealing for 60 h in various solvents.

The images were taken with polarizers set to 85°, which also allows the observation of non-bifringent structures at the surface. Besides the crystalline structures which are present in all samples shown in Figure 2, additional amorphous parts are noticed within the samples annealed in water, EtOH, and IPA. For the water sample, large flat areas remain, showing that the time frame was not sufficient to achieve full crystallization. In the alcohols, a dewetting of the sample is present; within the droplets, single crystals of clotrimazole form, but similar to water not all of the material crystallized in the investigated time frame.

For the identification of the crystalline structure, X-ray diffraction experiments are performed on the vapor annealed thin films (see Figure 3). As a specular geometry is used, only net planes lying parallel to the glass surface are accessible. This allows on the one hand the crystalline structure to be elucidated and on the other hand preferred alignment to be determined. The samples shown in Figure 2 reveal X-ray patterns (Figure 3) with various peaks over the entire scan range. The most prominent peaks are located at 2θ = 9.20°, 9.87°, 12.46°, and 18.63° corresponding to the 001, $0\bar{1}1$, $1\bar{1}0$, and 002 net-planes of the single crystal structure[23,34] with a = 0.876 nm, b = 1.055 nm, c = 1.060 nm, α = 114.1°, β = 97.0°, γ = 97.5°. Within the limit of accuracy, it can be concluded that solvent incorporation within the crystal does not take place or is of minor importance. The broad increase in intensity at large angles is due to the amorphous glass substrates. Amorphous fractions of clotrimazole have a very low diffraction signal due to the small thickness of the film and are below the detection limit within this experiment. The variation in the peak height is a result of changing textures, that is, the net planes that are in contact with the substrate surface. The sample annealed within XYL results in only one netplane being in contact with the surface. This follows from the fact that only two peaks, that is, 001 and 002, are visible within the spectra. Most other samples show various directions with a slight favor for the 001 direction, but the sample annealed in water shows a favorization of the $0\bar{1}1$ contact plane. The MeCN annealed sample shows a similar peak height for both, suggesting both directions equally likely.

For sake of completeness, the X-ray pattern of a sample vapor annealed in THF is shown revealing no diffraction peaks; that is, crystallization did not take place during the exposure to the THF vapor (see Figure 3 bottom curve). The optical microscopy image of these samples does not show any bifringent structures in accordance with their solid state being amorphous.

Surprisingly, deposition of clotrimazole via drop casting from XYL and TOL reveal the formation of "spontaneously" formed crystallites. The same experiments performed on the other systems did not reveal crystalline structure, and amorphous films remained at the glass surface after solvent removal. A drop cast experiment is performed via setting a defined drop of 100 μL solution on top of a 2.5 × 2.5 cm^2 glass slide and covered with a Petri dish. After the solvent removal, which took about 15 to 30 min, which is much longer compared to the spin coating process, measurements were performed. Optical micrographs of drop casted clotrimazole films from XYL (Figure 4a) and TOL (Figure 4b) solutions reveal crystallites after solvent evaporation. While the xylene sample contains large crystals of elongated shapes together with some amorphous fractions, the toluene sample contains two distinct morphologies; spherulite structures cover nearly the entire surface, while large elongated crystallites are distributed over the surface. Amorphous fractions of clotrimazole are not noticeable. Corresponding X-ray diffraction experiments reveal various peaks for both samples over the scan range.

DISCUSSION

Deposition of clotrimazole via spin coating from toluene results in amorphous films which prevail for a long period of time. As the molecules are complex and asymmetric with the four rings being rotated around each other (see Figure 1), the assembling into a low energy crystalline state is slowed; the molecules need

dx.doi.org/10.1021/cg401859p | *Cryst. Growth Des.* 2014, 14, 1386−1391

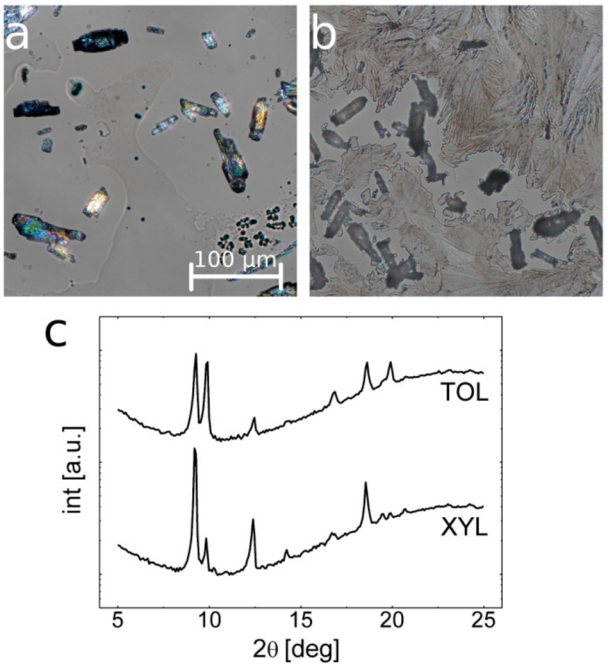

Figure 4. Optical micrographs (polarizers set to 85°) of clotrimazole drop cast from *p*-xylene (a) and toluene (b) solution onto glass surfaces. Corresponding X-ray diffraction patterns of the two samples (c).

to translate as well as to rotate to stick onto adjacent molecules, which in the amorphous state is strongly hindered. Anyway, by drop casting nearly spontaneous crystallization is observed for samples prepared from XYL and TOL solutions. Within other solvents, a rapid crystallization is absent. This, on the one hand, is a result of the two solvents (XYL and TOL) having good solvent conditions for clotrimazole, which enhances the molecular movement in the solution. On the other hand, these two solvents have the lowest vapor pressure compared to all other solvents (compare within Table 1) meaning solvent evaporation is slow. This leaves more time for assembling, as

Table 1. List of the Dispersive (δ_d), Polar (δ_p), H-Bonding (δ_h) Hansen-Solubility Parameters (HSPs for solvents,[35] mean value for SiO_x[27] and Clotrimazole[37]) Together with the Solubility Parameter Distance for Solvent−Clotrimazole Combinations[a]

	HSP			Ra			cryst	
mater	δ_d	δ_p	δ_h	Clot.	SiO_x	p_v [torr]	dc	va
H_2O	15.5	16.0	42.3	41.7	23.3	23.7[37]	na	+
MeOH	15.1	12.3	22.3	24.0	10.7	126.9[37]	−	+
EtOH	15.8	8.8	19.4	19.9	13.4	58.8[37]	−	+
IPA	15.8	6.1	16.4	17.2	16.5	43.7[37]	−	+
XYL	17.6	1.0	3.1	9.4	27.0	8.3[37]	+	+
TOL	18.0	1.4	2.0	8.8	27.4	28.4[37]	+	+
DMK	15.2	7.4	4.8	14.0	21.4	229.5[37]	−	+
MeCN	15.3	18.0	6.1	19.5	14.9	91.2[37]	−	+
THF	16.8	5.7	8.0	11.1	20.2	162.2[37]	−	−
SiO_x	17	22	20	25.7	0.0	−		
Clot.	22.0	3.9	4.6	0.0	25.8	−		

[a]Additionally, the viscosity (η) and the vapor pressure (p_v) are listed. Last two columns indicate if crystallization was observed (+) or was not (−) for the drop cast (dc) and vapor annealed (va) samples.

the concentration changes on evaporation are not as rapid. The XRD investigations reveal that these crystals have no preferred orientation with respect to the surface, which suggests that the crystallites form within the bulk solution rather than at the solid−liquid interface.

The amorphous film can be easily transformed into a crystalline film by solvent annealing in eight different solvent vapors, and within one, namely, THF, the film remained amorphous (compare within Table 1). Various morphologies result, whereby similarities between certain samples exist. For the understanding of the formed shapes, the HSPs of the various substances are compared (see Table 1). In general, the HSPs describe the cohesive energy density that is present within a substance. Furthermore, the energy is decomposed of three contributions according to the most common interactions, that is, the dispersive interactions (δ_d), polar interaction (δ_p), and the hydrogen bonding contributions (δ_h). This set of data, which can be found in the literature, allows estimating the nature of interaction which is responsible for the formation of certain morphologies. In addition, a set of HSPs represent a point in three-dimensional space which can be used to calculate the solubility parameter distance of two substances (Ra) via

$$\mathrm{Ra} = \sqrt{4(\delta_{d2} - \delta_{d1})^2 + (\delta_{p2} - \delta_{p1})^2 + (\delta_{h2} - \delta_{h1})^2}$$

In general, a smaller Ra value means that the affinity between different kinds of materials is increased, meaning that clotrimazole dissolves in the investigated substance. In addition, the adsorption affinity of molecules (API or solvent) in general is crucially influenced by the chemical composition. Silica is hydrophilic due to its silanol groups at the surface but has still a certain hydrophobic character due to the remaining SiO_x groups. Consequently, a water contact angle of about 35° is observed. Clotrimazole on the other hand is a hydrophobic molecule with a water contact angle of about 78°. This is also reflected in the respective Ra values; for silica Ra = 23.3 is obtained, while the clotrimazole is nearly doubled with Ra = 41.7 meaning that the solvent favors the contact with the silica rather than the clotrimazole.

Within a vapor annealing experiment, the solvent is able to reach the clotrimazole-modified silica surface. Depending on the interactions (besides other parameters such as temperature or pressure) a certain amount of solvent is able to condensate at the clotrimazole film. Fractions of condensed solvent diffuse into the film and/or are able to reach the clotrimazole−silica interface. This condensation provides further the ability to dissolve the organic API up to the saturation limit which may assist in the crystallization process.

Spherulite-like crystallization is observed for an amorphous sample which is exposed to a water atmosphere. The X-ray scan reveals that the sample has a preferred $0\bar{1}1$ contact plane with the surface. During vapor annealing, water droplets condense on the amorphous and smooth clotrimazole surface with a contact angle of around 78°. The solubility of clotrimazole in water is very low due to the very high polar and H-bonding contributions (see Table 1). Fast supersaturation therefore results within the droplets, and crystallization seeds are more likely to form. For the spontaneously formed nuclei at the sample surface, additional molecules are accessible, and the formation of crystallites takes place at the clotrimazole−air interface. Spherulitic structures are typically a result of a single nuclei initiating crystallization in various directions along the

dx.doi.org/10.1021/cg401859p | *Cryst. Growth Des.* 2014, 14, 1386−1391

surface simultaneously, and as the film is thin, molecules along the surface adapt their position only slightly. This results in spherulite arms with a common center. At larger spherulite sizes, the diffusion distance for additional molecules is increased, and a depletion zone forms close to the edge of the spherulites reducing the crystallization velocity. After the 60 h, the film still contained amorphous fractions. Thus, the diffusion process is slow, and the amount of crystal seeds forming is low.

At elevated temperatures of 70 °C, the molecules have more energy, which results in their diffusity being enhanced. In addition, higher temperatures mean that the solubility is increased. Both effects influence the morphology from spherulite type growth to barlike shaped (compare Figure 2, panels a and b). The different colors of the film indicate that the crystal extensions from the surface are enhanced, which indicate that diffusion in all three dimensions exists. This is also reflected in the XRD pattern which shows a preferred 001 texture, meaning crystals growth along other crystal directions, and most likely the growth is initiated at the silica−clotrimazole interface.

Comparing the HSPs of the alcohols with that of water shows that the polar and H-bonding contributions are significantly smaller; thus, the interaction probability with clotrimazole is enhanced; the Ra values are 24, 20, and 17 for MeOH, EtOH, and IPA, respectively. In addition, the Ra values calculated for the interaction strength with silica reveal much lower values ranging from 10 to 16. This means that the solubility of clotrimazole in the alcohols is higher and that the solvents have a strong affinity to the surface. This is reflected in the morphology within the vapor annealed film, which shows a dewetting structure. The initial solvent molecules are able to penetrate the film and to reach the silica−clotrimazole interface, reducing the interaction strength of the film. On account of their differences in their polar and hydrogen bonding character, the clotrimazole film reduces its surface area with respect to SiO_x. Within this dewetted droplike structure, the amorphous clotrimazole forms single nuclei resulting in large single crystals.

XYL and TOL have very similar HSPs and small Ra values, which suggests that good solvent properties for clotrimazole are present. Surprisingly, slight deviations of the surface morphology exist. Within XYL samples, the single crystalline structures are evident, while the TOL sample shows rodlike structures but additionally approaches diffusion limited aggregation (DLA) structures. DLA results typically from molecules not being able to diffuse along the crystal to low energetic facets and on the crystallization adapt a crystal site that is adjacent. Hence, a structure that deviates from the rodlike growth results. Most likely, leaving the system more time for the crystallization process would result in rodlike structures. Anyway, strong deviations of the vapor pressures are present for the two solvents with the vapor pressure of TOL being 3.5 times larger. A higher vapor pressure means that the bulk solvent has a stronger affinity to escape into the vapor phase, which results in strong fluctuation of the local concentration and therefore in rapid crystallization.

Within the DMK and MeCN samples, the morphologies are of DLA type with the branches being denser in the MeCN sample. The HSPs of these two solvents show significantly lower dispersive and higher polar/H-bonding contributions, which results in the Ra values being larger. From this follows that they exhibit a lower solvent quality with respect to TOL or XYL. This, together with the even higher vapor pressures, reduces their ability to promote molecular movements of clotrimazole, and thus the DLA results.

In THF and $MeCl_2$ vapor crystallization was not observed. The Hansen parameters suggest a similar nucleation should be present compared to the XYL and TOL. Anyway, THF and $MeCl_2$ have a much higher vapor pressure compared to most of the other solvents investigated. This means a higher concentration of the solvent molecules is present in the vapor phase which further promotes condensation on the clotrimazole film. From the parameter set a high solubility of clotrimazole is expected. The large amount of solvent condensed at the thin film together with good solvent quality reduces the probability to form nuclei or crystal grains of sufficient expansion required for the development of crystal growth.

■ CONCLUSION

Amorphous clotrimazole thin films are prepared via spin coating, and crystallization is successfully induced by solvent vapor annealing in a time frame of 60 h, which is significant faster compared to ambient crystallization that takes up to 10 days. Depending on the physicochemical properties of the chosen solvents, different crystal morphologies are obtained. These differences can be correlated with the interaction of the solvent with the amorphous clotrimazole thin film and the glass substrate and are reflected in the HSPs. With poor agreement of the HSP values for the investigated solvent and clotrimazole, spherulite-like structures form. A high affinity for the surface results in dewetting structures, while good agreement of the HSP results in single crystals or DLA, depending on the vapor pressure of the solvent used.

■ AUTHOR INFORMATION

Corresponding Author

*E-mail: oliver.werzer@uni-graz.at.

Notes

The authors declare no competing financial interest.

■ ACKNOWLEDGMENTS

The work was funded by the Austrian Science Fund (FWF): [P25541-N19]. E.R. thanks the NAWI Graz.

■ REFERENCES

(1) Van Eerdenbrugh, B.; Baird, J. A.; Taylor, L. S. *J. Pharm. Sci.* **2010**, *99* (9), 3826−3838.
(2) Newman, A. W.; Byrn, S. R. *Drug Discovery Today* **2003**, *8* (19), 898−905.
(3) Mosharraf, M.; Nyström, C. *Int. J. Pharmaceut.* **1995**, *122* (1−2), 35−47.
(4) Patel, V. R.; Agrawal, Y. K. *J. Adv. Pharm. Technol. Res.* **2011**, *2*, 81−87.
(5) Wojnarowska, Z.; Grzybowska, K.; Hawelek, L.; Dulski, M.; Wrzalik, R.; Gruszka, I.; Paluch, M. *Mol. Pharmaceutics* **2013**, *10*, 3612−3627.
(6) Gupta, M. K.; Vanwert, A.; Bogner, R. H. *J. Pharm. Sci.* **2003**, *92*, 536−551.
(7) Rustichellia, C.; Gamberinia, G.; Feriolia, V.; Gamberinia, M. C.; Ficarrab, R.; Tommasini, S. *J. Pharm. Biomed. Anal.* **2000**, *23*, 41−54.
(8) Griesser, U. J.; Burger, A.; Mereiter, K. *J. Pharm. Sci.* **1997**, *86*, 352−358.
(9) Cordeiro, N.; Aurenty, P.; Belgacem, M. N.; Gandini, A.; Neto, C. P. *Journal of Colloid and Interface Science* **1997**, *187* (2), 498−508.

(10) Holt, R.; Newman, R. *Journal of Clinical Pathology* **1972**, *25* (12), 1089−1097.
(11) Werzer, O.; Kunert, B.; Roblegg, E.; Zimmer, A.; Oehzelt, M.; Resel, R. *Cryst Growth Des* **2013**, *13* (3), 1322−1328.
(12) Lee, D.-J.; Lee, S.; Kim, I. W. *Int. J. Mol. Sci.* **2012**, *13*, 10296−10304.
(13) Pardeike, J.; Weber, S.; Haber, T.; Wagner, J.; Wagner, J.; Zarfl, H. P.; Plank, H.; Zimmer, A. *Int. J. Pharmaceutics* **2011**, *419*, 329−338.
(14) Arya, A.; Chandra, A.; Sharma, V.; Pathak, K. *Int. J. ChemTech Res.* **2010**, *2* (1), 576−583.
(15) Active pharmaceutical ingredient adsorbed on solid support. EP Patent 2,238,979, 2010.
(16) Werzer, O.; Stadlober, B.; Haase, A.; Flesch, H.-G.; Resel, R. *Eur. Phys. J. Appl. Phys.* **2009**, *46*, 20403(1−5).
(17) Werzer, O.; Stadlober, B.; Haase, A.; Oehzelt, M.; Resel, R. *Eur. Phys. J. B* **2008**, *66*, 455−459.
(18) Moser, A.; Novak, J.; Flesch, H. G.; Djuric, T.; Werzer, O.; Haase, A.; Resel, R. *Appl. Phys. Lett.* **2011**, *99*, No. 221911.
(19) Resel, R. *J. Phys.: Condens. Matter* **2006**, *20*, 184009(1-10).
(20) Tettenborn, D. *Naunyn-Schmiedeberg's Arch. Pharmacol.* **1970**, *266* (4), 468−469.
(21) Pandey, R.; Ahmad, Z.; Sharma, S.; Khuller, G. K. *Int. J. Pharm.* **2005**, *301* (1−2), 268−276.
(22) Sawyer, P. R.; Brogden, R. N.; Pinder, R. M.; Speight, T. M.; Avery. *Drugs* **1975**, *9* (6), 424−447.
(23) Song, H.; Shin, H. S. *Acta Crystallogr., Sect. C: Cryst. Struct. Commun.* **1998**, *54*, 1675−1677.
(24) Yong, C. S.; Li, D. X.; Prabagar, B.; Park, B. C.; Yi, S. J.; Yoo, B. K.; Lyoo, W. S.; Woo, J. S.; Rhee, J. D.; Kim, J. A.; Choi, H. G. *Pharmazie* **2007**, *62* (10), 756−759.
(25) Golin, J.; Kon, Z. N.; Wu, C. P.; Martello, J.; Hanson, L.; Supernavage, S.; Ambudkar, S. V.; Sauna, Z. E. *Biochemistry* **2007**, *46* (45), 13109−13119.
(26) Gu, C.-H.; Grant, D. J. W. *J. Pharm. Sci.* **2001**, *90* (9), 1277−1287.
(27) Lafaurie, A.; Azema, N.; Ferry, L.; Lopez-Cuesta, J. M. *Powder Technol.* **2009**, *192* (1), 92−98.
(28) Miller, S.; Fanchini, G.; Lin, Y.-Y.; Chen, C.-W.; Su, W.-F.; Chhowalla, M. *J. Mater. Chem.* **2008**, *18* (3), 306−312.
(29) Dickey, K. C.; Anthony, J. E.; Loo, Y. L. *Advanced Materials* **2006**, *18* (13), 1721−1726.
(30) Conboy, J. C.; Olson, E. J.; Adams, D. M.; Kerimo, J.; Zaban, A.; Gregg, B. A.; Barbara, P. F. *J. Phys. Chem. B* **1998**, *102* (23), 4516−4525.
(31) Hansen, C. M. *J. Pain Technol.* **1967**, *39*, 104−117.
(32) Schubert, D. W.; Dunkel, T. *Mater. Res. Innovations* **2003**, *5*, 314−321.
(33) Birkholz, M. *Thin Film Analysis by X-ray Scattering*; Wiley: New York, 2006.
(34) Das, S.; Ng, W. K.; Tan, R. B. H. *Eur. J. Pharm. Sci.* **2012**, *47* (1), 139−151.
(35) Hansen, C. *Hansen Solubility Parameters: A user's handbook,* 2nd ed. CRC Press: Boca Raton, 2007.
(36) Thakral, S.; Thakral, N. K. *J. Pharm. Sci.* **2013**, *102*, 2254−2263.
(37) D.D.D.B., http://ddbonline.ddbst.de/AntoineCalculation/AntoineCalculationCGI.exe?component=Ethanol (accessed 10.10.2013).